International Journal of Computational and Theoretical Chemistry
2017; 5(6): 59-68
http://www.sciencepublishinggroup.com/j/ijctc
doi: 10.11648/j.ijctc.20170506.12
ISSN: 2376-7286 (Print); ISSN: 2376-7308 (Online)

A Quantum-chemical Study of the Relationships Between Electronic Structure and Anti-proliferative Activity of Quinoxaline Derivatives on the HeLa Cell Line

Gaston Assongba Kpotin[1, *], Juan Sebastián Gómez-Jeria[2]

[1]Department of Chemistry, Faculty of Sciences and Technologies, University of Abomey-Calavi, Abomey-Calavi, Republic of Benin

[2]Quantum Pharmacology Unit, Department of Chemistry, Faculty of Sciences, University of Chile, Santiago, Chile

Email address:

gaston.kpotin@fast.uac.bj (G. A. Kpotin)

[*]Corresponding author

To cite this article:

Gaston Assongba Kpotin, Juan Sebastián Gómez-Jeria. A Quantum-chemical Study of the Relationships Between Electronic Structure and Anti-proliferative Activity of Quinoxaline Derivatives on the HeLa Cell Line. *International Journal of Computational and Theoretical Chemistry.* Vol. 5, No. 6, 2017, pp. 59-68. doi: 10.11648/j.ijctc.20170506.12

Received: November 28, 2017; **Accepted**: December 9, 2017; **Published**: January 11, 2018

Abstract: A study of the relationships between electronic structure and anti-proliferative activity of quinoxaline derivatives on the HeLa cell line was carried out. For this QSAR study the technique employed is the Klopman-Peradejordi-Gómez (KPG) method. We obtain a statistically significant equation (R= 0.97 R^2= 0.94 adj-R^2= 0.91 F (8, 15)=29.50 p<0.000001 and SD=0.06). The results showed that the variation of the activity depends on the variation of the values of eight local atomic reactivity indices. The process seems to be charge and orbital-controlled. Based on the analysis of the result, a partial two-dimensional pharmacophore was built. The results should be useful to propose new molecules which higher activity.

Keywords: Quinoxaline, HeLa Cell Line, KPG Method, QSAR, Pharmacophore, DFT

1. Introduction

Hela is the first immortalized cell line [1]. This cell line originates from a cervical cancer tumor of a patient named Henrietta Lacks, who later died of her cancer in 1951 [1]. One of the earliest uses of HeLa cells was to develop the vaccine against the polio virus [2]. The genomic and transcriptomic resource for a HeLa cell line based on deep DNA and RNA sequencing was created in 2013 [3]. Several studies are performed to found molecules that inhibit the proliferation of this cell line [4–28]. Theoretical studies were also done and are useful to explain the mechanism, the affinity and the activities of different compounds [26–29]. This work presents the results of the use of the KPG method [30] to obtain quantitative relationships between the electronic structure of quinoxaline derivatives and their anti-proliferative activities on the HeLa cell line.

2. Methods, Models and Calculations

2.1. Methods and Models

For this study we use the Klopman-Peradejordi-Gomez (KPG) method. In 1967, Klopman and Hudson presented a general perturbation model for chemical reactivity including ionic interactions and not restricted only to π electron [31–33]. In their model, the electronic energy change, ΔE, associated with the interaction of atom i of molecule A with atom j of molecule B is given by:

$$\Delta E = \sum_p \left[Q_i Q_j / R_{ij} + (1/2)(\beta_{ij}^2) \sum_m \sum_n F_{mi} F_{n'j} / (E_m - E_{n'}) - (1/2)(\beta_{ij}^2) \sum_{m'} \sum_n F_{m'i} F_{nj} / (E_{m'} - E_n) \right] \quad (1)$$

where Q_i is the net charge of atom I, F_{mi} is the Fukui index of OM m of atom i, β_{ij} is the resonance integral (assumed to be independent of the kind of atomic orbitals (OA) because the A-B complex does not involve covalent bonds), E_m ($E_{m'}$)

is the energy of the m-th occupied MO (m' for the empty MOs) of molecule A. n and n' refer to molecule B. The summation on p is over all interacting atom pairs. The first term of the right side of Equation 1 represents the electrostatic interaction between atom with net charges Q_i and Q_j. The next two terms introduce the interactions between occupied MOs of one molecule with the empty MOs of the other molecule and vice versa. As this model represents the interaction energy in terms of atom-atom interactions, it was only a matter of time that someone applied it for pharmacological/biological problems. Then, in 1971, Peradejordi et al published an article where they presented the results of a quantum-chemical study of the structure-activity relationships of tetracycline antibiotics [34]. The authors proposed that the inhibitory rate constants, K_i^I, can be expressed as:

$$\log K_i^I = cons\tan t + \log K_i^c \quad (2)$$

where K_i^c is the ribosome-tetracycline equilibrium constant. Now, let us consider the state of thermodynamic equilibrium and a 1:1 stoichiometry in the formation of the drug-receptor complex:

$$D_i + R \rightleftarrows D_iR \quad (3)$$

where D_i is the drug, R the receptor and D_iR the drug-receptor complex. According to statistical thermodynamics the equilibrium constant K_i is written as:

$$K_i = \frac{Q_{D_iR}}{Q_{D_i}Q_R}\exp(-\Delta\varepsilon_0^i/kT) \quad (4)$$

where Q_{D_iR}, Q_{D_i} and Q_R are respectively the total partition functions of the drug-receptor complex, the drug and the receptor; k is the Boltzmann's constant and T is the absolute temperature. $\Delta\varepsilon_0^i$ is the difference between the ground-state energy of D_iR and the energies of the ground-states of D_i and R:

$$\Delta\varepsilon_0^i = \varepsilon_{D_iR} - (\varepsilon_{D_i} + \varepsilon_R) \quad (5)$$

Peradejordi et al consider that the partition function terms and the solvation energy are constant. After overs considerations and approximations (for details see [34]), the linear equations is obtained:

$$\log K_i^I = A + \sum_p \left\{ a_p Q_{b,p} + b_p S_{b,p}^E + c_p S_{b,p}^N \right\} \text{ i=1,2,…,n} \quad (6)$$

where A, a_p, b_p, c_p are constant to be determined $Q_{b,p}$ is the net charge $S_{b,p}^E$ is the total atomic electrophilic superdelocalizability of atom p and $S_{b,p}^N$ is the total atomic nucleophilic superdelocalizability of atom p. Gómez-Jeria continued working the drug-site interaction energy and published the results [35–43]. In 2013, he derived the following equation [44]:

$$\log(IC_{50}) = a + bM_{D_i} + c\log\left[\sigma_{D_i}/(ABC)^{1/2}\right] + \sum_j \left[e_j Q_j + f_j S_j^E + s_j S_j^N \right] +$$
$$\sum_j \sum_m \left[h_j(m) F_j(m) + x_j(m) S_j^E(m) \right] + + \sum_j \sum_{m'} \left[r_j(m') F_j(m') + t_j(m') S_j^N(m') \right] \quad (7)$$
$$+ \sum_j \left[g_j \mu_j + k_j \eta_j + o_j \omega_j + z_j \varsigma_j + w_j Q_j^{\max} \right]$$

where a, b and c are constants, M_{D_i} is the drug's mass, σ_{D_i} its symmetry number and ABC the product of the drug's moments of inertia about the three principal axes of rotation. Q_j is the net charge of atom j, S_j^E and S_j^N are, respectively, the total atomic electrophilic and nucleophilic superdelocalizabilities of Fukui et *al.*, $F_{j,m}$ ($F_{j,m'}$) is Fukui index of the occupied (vacant) MO m(m') located on atom j. $S_j^E(m)$ is the atomic electrophilic superdelocalizability of MO m on atom j, etc. The total atomic electrophilic superdelocalizability of atom j corresponds to the sum over occupied MOs of the $S_j^E(m)$'s and the total atomic nucleophilic superdelocalizability of atom j is the sum over vacant MOs of $S_j^N(m')$'s. μ_j is the local atomic electronic chemical potential of atom j, η_j is the local atomic hardness of atom j, ω_j is the local atomic electrophilicity of atom j, ς_j is the local atomic softness of atom j, and $Q_j^{\max}$ is the maximum amount of electronic charge that atom j may accept from another site. O_k 's are the orientational parameters of the substituents. Throughout this paper $HOMO_j^*$ refers to the highest occupied molecular orbital localized on atom j and $LUMO_j^*$ to the lowest empty MO localized on atom j.

$$\text{with } \log\left[(ABC)^{-1/2}\right] \simeq \sum_t \sum_t m_{i,t} R_{i,t}^2 = \sum_t O_t \quad (8)$$

where the summation over t is over the different substituents of the molecule, $m_{i,t}$ is the mass of the i-th atom belonging to the t-th substituent, $R_{i,t}$ being its distance to the atom to which the substituent is attached. This approximation allows him to transform a molecular property into a sum of substituent properties. He proposed that these terms represent

the fraction of molecules attaining the proper orientation to interact with a given site. He called them Orientational Parameters (OP). The new local atomic reactivity indices (LARIs) of Eq. 7 are defined as follows:

Local atomic electronic chemical potential:

$$\mu_i = (\varepsilon_{HOMO^*,i} + \varepsilon_{LUMO^*,i})/2 \quad (9)$$

Local atomic hardness:

$$\eta_i = (\varepsilon_{HOMO^*,i} - \varepsilon_{LUMO^*,i}) \quad (10)$$

Local electrophilic superdelocalizability of the HOMO* of atom i and local nucleophilic superdelocalizability of the LUMO* of atom i:

$$S_i^{E^*} = \frac{F_{i,HOMO^*}}{\varepsilon_{HOMO^*}} \quad (11)$$

$$S_i^{N^*} = \frac{F_{i,LUMO^*}}{\varepsilon_{LUMO^*}} \quad (12)$$

Local atomic softness of atom i:

$$S_i = \frac{1}{\eta_i} \quad (13)$$

Local atomic electrophilicity of atom i:

$$\omega_i = \frac{\mu_i^2}{2\eta_i} \quad (14)$$

The maximal amount of charge atom i may receive:

$$Q_i^{\max} = -\frac{\mu_i}{\eta_i} \quad (15)$$

The physical meaning of these indices is summarized in Table 1.

Table 1. *Local Atomic Reactivity Indices and their physical meaning [44].*

Index	Name	Physical meaning
Q_i	Net atomic charge of atom i	Electrostatic interaction
S_i^E	Total atomic electrophilic superdelocalizability of atom i	Total atomic electron-donating capacity of atom i (MO-MO interaction)
S_i^N	Total atomic nucleophilic superdelocalizability of atom i	Total atomic electron-accepting capacity of atom i (MO-MO interaction)
$S_i^E(m)$	Orbital atomic electrophilic superdelocalizability of atom i and occupied MO m	Electron-donating capacity of atom i at occupied MO m (MO-MO interaction)
$S_i^N(m')$	Orbital atomic nucleophilic superdelocalizability of atom i and empty MO m’	Electron-accepting capacity of atom i at empty MO m’ (MO-MO interaction)
F_i	Fukui index of atom i	Total electron population of atom i (MO-MO interaction)
F_{mi}	Fukui index of atom i and occupied MO m.	Electron population of occupied MO m at atom i (MO-MO interaction)
$F_{m'i}$	Fukui index of atom i and empty MO m’	Electron population of empty MO m’ at atom i (MO-MO interaction)
μ_i	Local atomic electronic chemical potential of atom i	Propensity of atom i to gain or lose electrons
η_i	Local atomic hardness of atom i	Resistance of atom i to exchange electrons with a site
ς_i	Local atomic softness of atom i	The inverse of μ_i
ω_i	Local atomic electrophilicity of atom i	Propensity of atom i to receive extra electronic charge together with its resistance to exchange charge with a site
$Q_i^{\max}$	Maximal amount of electronic charge atom i may receive	Maximal amount of electronic charge that atom i may receive from a donor site

The Klopman-Peradejordi-Gómez (KPG) method is also discussed in many previous papers [30, 35, 36, 38, 39, 42, 44–46]. From a conceptual perspective, the work presented here is a test of the hypothesis stating that the KPG model can provide a quantitative and formal relationship between the molecular structure and any biological activity. Nowadays, the KPG model produced excellent results in all its applications[35, 44, 46–53].

2.2. Selection of Molecules

For this study, a series of quinoxline derivatives were selected [23]. These molecules have an anti-proliferative activity on the HeLa cell line. The experimental data was taken from a recent study [23]. The structures of the

compounds are shown in Figure 1 and Table 2 which also summarizes the values of their median inhibitory concentrations expressed as $\log(IC_{50})$.

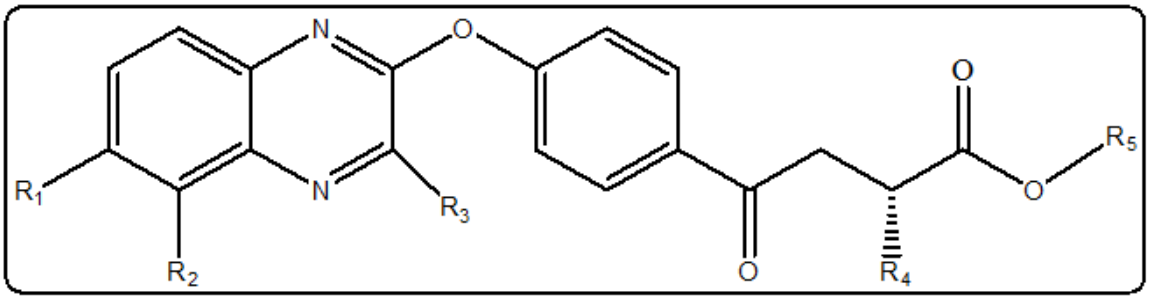

Figure 1. *Structure of quinoxaline derivatives.*

Table 2. *Quinoxalines and their experimental anti-proliferative activity.*

Mol.	R_1	R_2	R_3	R_4	R_5	$\log(IC_{50})$
1	H	H	CH_3	CH_3	CH_3	1.66
2	H	H	CH_3	$(CH_3)_2CHCH_2$-	CH_3	1.35
3	H	H	CH_3	$CH_3CH_2CH(CH_3)$-	CH_3	1.58
4	H	Cl	CH_3	CH_3	CH_3	1.42
5	H	Cl	CH_3	$(CH_3)_2CHCH_2$-	CH_3	1.51
6	Cl	H	CH_3	$C_6H_5CH_2$-	CH_3	1.44
7	Cl	H	CH_3	$(CH_3)_2CHCH_2$-	CH_3	1.34
8	H	H	CH_3	CH_3	H	1.45
9	H	H	CH_3	$(CH_3)_2CHCH_2$-	H	1.29
10	H	H	CH_3	$CH_3CH_2CH(CH_3)$-	H	1.48
11	H	Cl	CH_3	CH_3	H	1.32
12	H	Cl	CH_3	$(CH_3)_2CHCH_2$-	H	1.33
13	Cl	H	CH_3	$C_6H_5CH_2$-	H	1.33
14	Cl	H	CH_3	$(CH_3)_2CHCH_2$-	H	1.16
15	H	H	$NH(CH_2)_{11}CH_3$	$C_6H_5CH_2$-	CH_3	1.48
16	H	H	$NH(CH_2)_{11}CH_3$	CH_3	CH_3	1.43
17	H	H	$NH(CH_2)_{11}CH_3$	$(CH_3)_2CHCH_2$-	CH_3	1.49
18	H	H	$NH(CH_2)_{11}CH_3$	H	CH_3	1.63
19	H	H	$NHC(CH_2)_3$	CH_3	CH_3	1.59
20	H	H	$NHC(CH_2)_3$	$C_6H_5CH_2$-	CH_3	1.01
21	H	H	$NH(CH_2)_{11}CH_3$	$C_6H_5CH_2$-	H	0.87
22	H	H	$NH(CH_2)_{11}CH_3$	CH_3	H	0.52
23	H	H	$NH(CH_2)_{11}CH_3$	$(CH_3)_2CHCH_2$-	H	1.33
24	H	H	$NH(CH_2)_{11}CH_3$	H	H	1.42
25	H	H	$NHC(CH_2)_3$	CH_3	H	1.26
26	H	H	$NHC(CH_2)_3$	$CH_3CH_2CH(CH_3)$-	H	1.63
27	H	H	$NHC(CH_2)_3$	$C_6H_5CH_2$-	H	1.18

2.3. Calculations

The electronic structure of each fully optimized molecule was obtained using the Density Functional Theory (DFT) at the B3LYP/6-31G (d, p) level with the Gaussian software [54]. The local atomic reactivity indices were calculated from the single point results of Gaussian03 using the D-Cent-QSAR software [55] with a correction for Mulliken populations [56]. All populations of electrons less than or equal to 0.01e are considered null [56]. The orientational parameters of the substituents are calculated in the usual manner [57, 58]. We have used the concept of common skeleton defined as a set of atoms common to all the molecules analyzed. We hypothesize that the variation of the numerical values of the local atomic reactivity indices (LARIs) of the atoms of this common skeleton accounts for almost all the variation of the biological activity. As the number of LARIs involved is greater that the number of molecules, the solving of the linear systems of equations is not possible. For this reason we employed the technique of multiple linear regression analysis (LMRA) to determine the

atoms that are directly involved in the variation of the biological activity. The data matrix contains log (IC_{50}) as a dependent variable, and the local indices of atomic reactivity of all the atoms of the common skeleton as independent variables. The Statistica 10 software was used to perform LMRA studies [59]. The numbering of the common skeleton atoms is shown in Figure. 2.

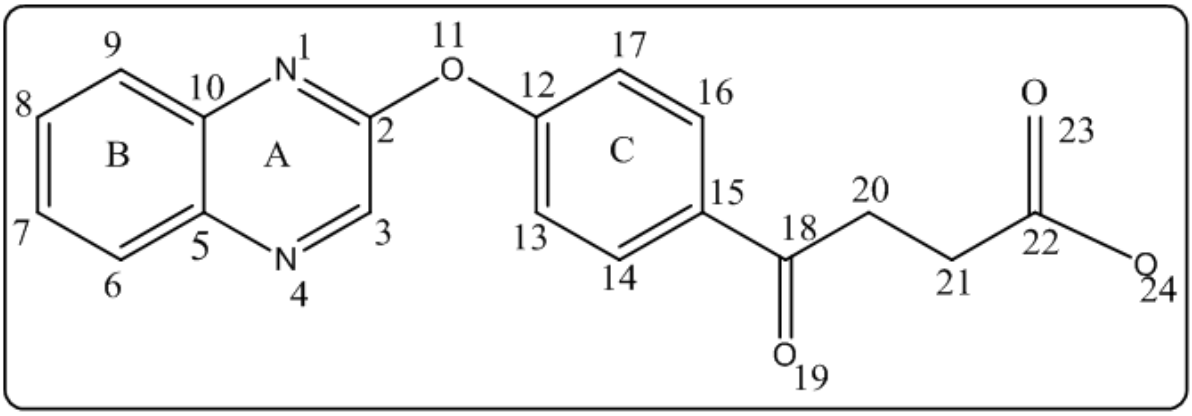

Figure 2. *Common skeleton numbering.*

3. Results

The best statistically significant equation obtained is the following:

$$\log(IC_{50}) = -33.32 + 1.69F_{21}(HOMO)^{*} - 2.61S_{21}^{E} + 0.04S_{16}^{N} - 78.05Q_{16} - 0.12F_{23}(HOMO)^{*} - 1.28F_{15}(LUMO)^{*} + 0.69F_{20}(HOMO)^{*} + 0.001S_{22}^{N}(LUMO)^{*} \quad (16)$$

with n=24, R= 0.97, R^2= 0.94, adj-R^2= 0.91, F(8.15)=29.50, ($p< 0.000001$) and a standard error of estimate of 0.06. No outliers were detected and no residuals fall outside the ±2σ limits. Here $F_{21}(HOMO)^{*}$ is the electron population (Fukui index) of the highest occupied MO localized on atom 21, S_{21}^{E} is the total atomic electrophilic superdelocalizability of atom 21, S_{16}^{N} is the total atomic nucleophilic superdelocalizability of atom 16, Q_{16} is the net charge of atom 16, $F_{23}(HOMO)^{*}$ is the Fukui index of the highest occupied MO localized on atom 23, $F_{15}(LUMO)^{*}$ is the Fukui index of the first lowest vacant MO localized on atom 15, $F_{20}(HOMO)^{*}$ is the electron population of the highest occupied MO localized on atom 20 and $S_{22}^{N}(LUMO)^{*}$ is the atomic nucleophilic superdelocalizability of the first lowest vacant MO localized on atom 22. Table 3 shows the beta coefficients and the t-test results for the significance of coefficients of equation 1. Concerning independent variables, Table 4 shows that the highest internal correlation is r^2[F_{20}(HOMO)*, F_{21}(HOMO)*]=0.43. Figure 3 shows the plot of observed values vs. calculated values of log(IC_{50}). The associated statistical parameters of Eq.16 show that this equation is statistically significant and that the variation of the numerical values of eight LARIs explains about 91% of the variation of the biological activity.

Table 3. *Beta coefficients and t-test for significance of coefficients in equation 1.*

	Beta	t(10)	p-level
$F_{21}(HOMO)^{*}$	0.70	7.44	<0.000002
S_{21}^{E}	-1.11	-10.08	<0.000000
S_{16}^{N}	0.97	7.67	<0.000001
Q_{16}	-0.43	-5.06	<0.0001
$F_{23}(HOMO)^{*}$	-0.26	-3.51	<0.003
$F_{15}(LUMO)^{*}$	-0.31	-3.26	<0.005
$F_{20}(HOMO)^{*}$	0.34	3.23	<0.006
$S_{22}^{N}(LUMO)^{*}$	0.28	2.61	<0.02

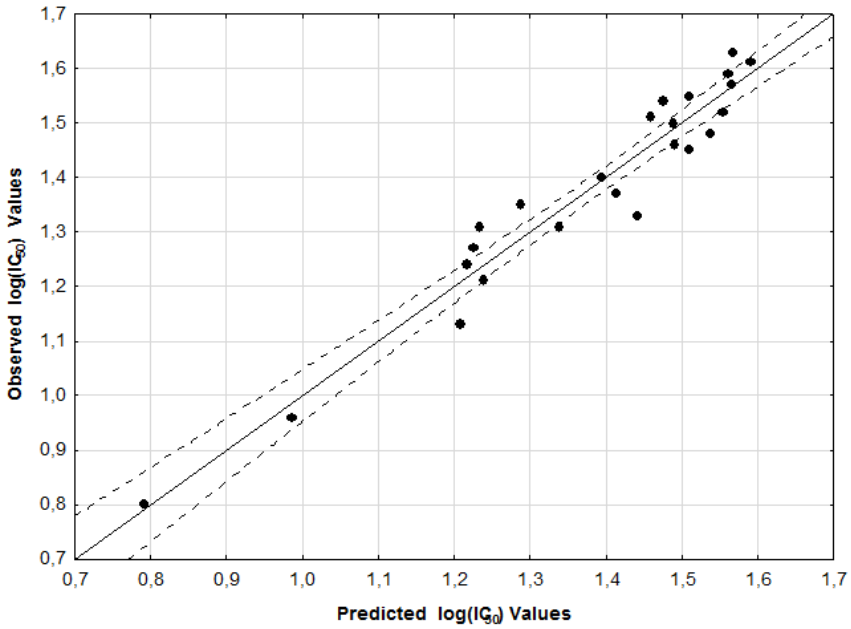

Figure 3. *Plot of predicted vs. observed log(IC50) values. Dashed lines denote the 95% confidence interval.*

Table 4. *Squared correlation coefficients for the variables appearing in equation 16.*

	$F_{21}(HOMO)^*$	S_{21}^E	S_{16}^N	Q_{16}	$F_{23}(HOMO)^*$	$F_{15}(LUMO)^*$	$F_{20}(HOMO)^*$
S_{21}^E	0.004	1.00					
S_{16}^N	0.02	0.3	1.00				
Q_{16}	0.002	0.034	0.2	1.00			
$F_{23}(HOMO)^*$	0.08	0.05	0.1	0.0001	1.00		
$F_{15}(LUMO)^*$	0.001	0.03	0.4	0.07	0.03	1.00	
$F_{20}(HOMO)^*$	0.4	0.06	0.00004	0.03	0.01	0.002	1.00
$S_{22}^N(LUMO)^*$	0.01	0.3	0.3	0.2	0.04	0.19	0.02

Local Molecular Orbitals

Tables 5 and 6 show the Local Molecular Orbitals of atom 5, 10, 20, 21, 22 and 23 (see Figure 3). Nomenclature: Molecule (HOMO) / (HOMO-2)* (HOMO-1)* (HOMO)* - (LUMO)* (LUMO+1)* (LUMO+2)*.

Table 5. *Local Molecular Orbitals of atoms 10, 15 and 20.*

Mol	Atom 10 (C)	Atom 15 (C)	Atom 20 (C)
1(96)	92π93π96π-97π98π99π	94π95π96π-97π98π100π	86σ90σ94σ-103σ107109
2 (108)	104π105σ108π-109π110π111π	106σ107π108π-109π110π112π	99σ100σ106σ-114σ115σ118σ
3 (116)	113σ115π116π-117π118π119π	114σ115π116π-117π118π120	107112σ114σ-122σ124σ127
4 (104)	101σ103π104π-105π106π107π	102σ103π104π-105π106π108π	93σ98σ102σ-112σ115σ118σ
5 (116)	113σ115π116π-117π118π119π	114σ115π116π-117π118π120π	107σ111σ114σ-122σ124σ127σ
6 (124)	118σ119σ122π-125π126π127π	120σ121π122π-125π126π128π	120σ121σ124σ-130σ132σ134σ
7 (116)	112σ113π116π-117π118π119π	114π115σ116π-117π118π120π	108σ111σ115σ-122σ124σ127σ
8 (92)	88π89σ92π-93π94π95π	90σ91π92π-93π94π96π	81σ86σ90σ-99σ100σ106σ
9 (104)	100π101σ104π-105π106π107π	102σ103π104π-105π106π108π	98σ101σ102σ-109σ110σ111σ
10 (104)	100π101σ104π-105π106π107π	102σ103π104π-105π106π108π	97σ98σ102σ-111σ112σ116σ
11 (100)	97σ99π100π-101π102π103π	98σ99π100π-101π102π104π	89σ94σ98σ-108σ110σ115σ
12 (112)	109σ111π112π-113π114π115π	110σ111π112π-113π114π116π	104σ106σ110σ-118σ120σ121σ
13 (120)	114σ115σ118π-121π122π123π	116σ117π118π-121π122π124π	110σ112σ116σ-126σ128σ130
14 (112)	109π110π112π-113π114π115π	110π111σ112π-113π114π116π	106110σ111σ-118σ120σ122σ
15 (164)	160σ162π164π-168π17π77π	160π162π164π-165π166π167π	158σ159σ163σ-169σ171σ173σ
16 (144)	142σ143π144π-148π150π159σ	142π143π144π-145π146π147π	125σ138σ141σ-151σ157σ163σ
17 (156)	154σ155π156π-160π162π171π	154σ155π156π-157π158π159π	145σ153σ154σ-161σ163σ166σ
18 (140)	138σ139π140π-144π146π167	138π139π140π-141π142π143π	119σ134σ137σ-147σ154σ161σ
19 (112)	109σ111π112π-116π118π122σ	110π111π112π-113π114π115π	106σ108σ110σ-119σ127σ128σ

Mol	Atom 10 (C)	Atom 15 (C)	Atom 20 (C)
20 (136)	132σ134π136π-140π143π144π	132π134π136π-137π138π139π	131σ132σ135σ-137σ141σ143σ
21 (160)	158π159π160π-164π168π174σ	156π158π160π-161π162π163π	152154σ155σ-165σ167σ169σ
22 (140)	138σ139π140π-144π146π155σ	138π139π140π-141π142π143π	134σ136σ137σ-147σ148σ162
23 (152)	150σ151π152π-156π158π168σ	150π151π152π-153π154π155π	146σ148σ149σ-157σ159σ160σ
24 (136)	134σ135π136π-140π142π148σ	134π135π136π-137π138π139π	132σ133σ134σ-143σ144σ157σ
25 (108)	106σ107π108π-112π114π119σ	106π107π108π-109π110π111π	102σ104σ105σ-115σ117σ123σ
26 (120)	118σ119π120π-124π126π133σ	118π119π120π-121π122π123π	114σ116σ117σ-125σ127σ129σ
27 (128)	124σ126π128π-132π136π141σ	124π126π128π-129π130π131π	120σ122σ123σ-133σ135σ137σ

Table 6. *Local Molecular Orbitals of atoms 21, 22 and 23.*

Mol.	Atom 21 (C)	Atom 22 (C)	Atom 23 (O)
1(96)	86σ90σ94σ-102σ105σ110σ	86π89π90π-102π103π105π	89π90π94π-102π111π138π
2 (108)	102σ103σ106σ-114σ120σ124σ	94σ101π102π-113π114π115π	102π103π106π-114π145π162π
3 (116)	111σ112σ114σ-122σ129σ130σ	109π111π112π-122π124σ126σ	111π112π114π-122π171π173π
4 (104)	93σ98σ102σ-110σ114σ119σ	93σ97π98π-110π112π114σ	98π100π102π-110π120σ147σ
5 (116)	107σ111σ114σ-122σ128σ133σ	102σ109π111π-122π124π126σ	111π112π114π-122π171π173π
6 (124)	117σ120σ124σ-130σ131σ132σ	115π117π120σ-130π131π132π	115π117π120π-130π131π132π
7 (116)	108σ111σ115σ-122σ128σ133σ	101σ109π111π-122π124π126σ	110π111π115π-122π171π173π
8 (92)	81σ86σ90σ-97σ98σ100σ	81σ84π86π-97π98π99π	84π86π90π-97π98π131π
9 (104)	97σ98σ102σ-109σ110σ114σ	96π97π98π-109π110π111π	97π98π102π-109π110π116π
10 (104)	97σ98σ102σ-110σ112σ114σ	94π97π98π-109π110π112σ	97π98π102π-109π110π142π
11 (100)	89σ94σ98σ-106σ110σ111σ	89σ91π94π-106π108π110σ	91π94π98π-106π140π142π
12 (112)	104σ106σ110σ-118σ123σ124σ	99π104π106π-118π120π121σ	106π107π110π-118π124π164π
13 (120)	112σ116σ120σ-126σ127σ128σ	107π110π112π-126π127π128π	110π112π116π-126π127π128π
14 (112)	105106111σ-118σ123σ124σ	104π105π106π-118π120π122σ	106π107π111π-118π124π164π
15 (164)	156σ159σ163σ-169σ170σ171σ	141σ153π156π-169π170π171π	153π156π159π-169π170π171π
16 (144)	125σ138σ141σ-149σ165σ167σ	125σ135π138π-149π151π155	135π138π141π-149π218π219π
17 (156)	145σ150σ151σ-161σ172180	132π147π150π-161π163π165	150π151π153π-161π242π247π
18 (140)	119σ134σ137σ-145σ149σ159	119π131π134π-145π147π154σ	131π134π137π-145π192π199π
19 (112)	99σ106σ110σ-117σ127σ128σ	99π104π106π-117π119π121σ	104π106π110π-117π127π154σ
20 (136)	128σ132σ135σ-141σ142σ143σ	121σ126128π-141π142π143π	130lpπ131π132π-141π142π143π
21 (160)	154σ155σ159σ-165σ166σ167σ	143π148π152π-165π166π167π	152154π155π-165π166π167π
22 (140)	120σ134σ137σ-145σ148σ150σ	128π129π134π-145π147π148π	129π134π137π-145π211π213π
23 (152)	142σ146σ149σ-157σ162σ166σ	135π142π146π-157π159π160π	142π146π149π-157π166π234π
24 (136)	115σ130σ133σ-141σ146σ162σ	106σ123π130π-141π143π144π	125π130π133π-141π183σ189σ
25 (108)	95σ102σ105σ-113σ117σ118σ	95σ99π102π-113π115π117σ	99π102π105π-113π157π159π
26 (120)	111σ114σ117σ-125σ129σ130σ	110π111π114π-125π127σ129σ	114π115π117π-125π177π180σ
27 (128)	120σ123σ127σ-133σ134σ135σ	115π117π120π-133π134π135π	120π122π123π-133π134π135π

4. Discussion

The HeLa inhibition mechanism is unknown. We have stated that "it is important to stress that our hypothesis covers multi-step (for example, in the n-th step molecules must cross a pore) and multimechanistic (for example, to cross the pore molecules must interact consecutively with j unknown sites) processes. Therefore it seems logical to state that a necessary condition to obtain good structure-activity relationships is that all the steps and all the mechanisms inside each step must be the same for all the group of molecules under study" [44]. If the molecules studied here employ multi-step and/or multimechanistic action mechanisms that are not exactly the same for all, we may expect that the linear multiple regression results contain sometimes variables whose interpretation seems contradictory.

The beta values shows that the importance of variables is $S_{21}^{E} > S_{16}^{N} > F_{21}(HOMO)^{*} > Q_{16} > F_{20}(HOMO)^{*} > F_{15}(LUMO)^{*} > S_{22}^{N}(LUMO)^{*} > F_{23}(HOMO)^{*}$. The process seems to be charge and orbital-controlled. A variable-by-variable analysis indicates that a good activity is associated with low negative numerical values of S_{21}^{E} (they are always negative) and Q_{16}, with low numerical values of $F_{21}(HOMO)^{*}$ and $F_{20}(HOMO)^{*}$ (their values are always positive) and with high numerical values for $F_{15}(LUMO)^{*}$ and $F_{23}(HOMO)^{*}$. If $S_{22}^{N}(LUMO)^{*}$ is positive, a high inhibitory activity is associated with low numerical values. If S_{16}^{N} is positive, a good activity is associated with low numerical values for this index.

Atom 21 is a carbon atom in the lateral chain of ring C (Figure 2). Table 6 shows that all local MO have σ nature. A low value of S_{21}^{E} indicates that atom 21 should interact with a sigma electron rich center through its empty sigma local MOs. Note that the local HOMO* and the local LUMO* do not coincide with the molecule's frontier MOs. The interactions can be of the σ-π or σ-σ kind. The σ-σ interaction may occur with the sigma MOs of the $-CH_2-$ groups of some amino acids. This coincides with the requirement of a low value for $F_{21}(HOMO)^{*}$. Atom 16 is a carbon atom in ring C (Figure 2). If S_{16}^{N} is positive, a high inhibitory activity is associated with low numerical values for this index. From the

definition of S_{16}^{N}, the dominant term is $S_{16}^{N}(LUMO)*$. Low numerical values are obtained by shifting upwards the energy of the empty MOs, making this atom a bad electron acceptor. Therefore, we suggest that atom 16 is interacting with an electron deficient center. On the other hand, Eq. 16 shows that a high inhibitory activity is related with a positive value for Q_{16}, fact that seems to be contradictory with the interaction with an electron deficient center. Examining Table II we may see that S_{16}^{N} is more significant than Q_{16}. Therefore, and as a first approximation, we shall not consider Q_{16}. Atom 20 is a carbon atom of the side chain of ring C (Figure 2). All local MOs have σ nature (Table 6). A low value for $F_{20}(HOMO)*$ suggests that atom 20 is probably interacting with a center rich in sigma electrons. Note that this condition is the same that the one for atom 21. Atom 22 is the carbon atom of the carboxylate moiety of the side chain of ring C (Figure 2). $(LUMO)_{22}{}^{*}$ is a π MO in all molecules (Table 6). A low value for $S_{22}^{N}(LUMO)*$ is associated with high inhibitory activity. This value is obtained by shifting upwards the $(LUMO)_{22}*$ eigenvalue and making the MO less reactive. So, we suggest that atom 22 is interacting with a π electron deficient center. Atom 15 is a carbon atom in ring C (Figure 2). $(LUMO)_{15}*$ is a MO of π nature (Table 5). A high value for $F_{15}(LUMO)*$ suggests that this lowest unoccupied local MO is interacting with an electron rich center. Atom 23 is an oxygen atom of the carboxylate moiety in the side chain of ring C (Figure 2). A high value for $F_{23}(HOMO)*$ suggests that the highest occupied local is interacting with an electron deficient center. All the above suggestions are shown in the partial 2D pharmacophore of Figure 4.

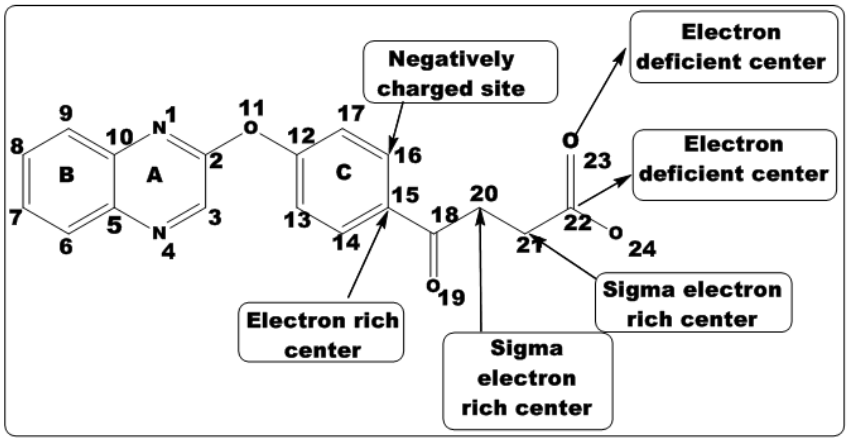

Figure 4. *Partial 2D pharmacophore for the anti-proliferative activities of quinoxaline derivatives on the HeLa cell line.*

5. Conclusion

We obtained a statistically significant relationship between the variation of the anti-proliferative activity of some quinoxaline derivatives and the variation of the numerical values of a set of local atomic reactivity indices. This allowed us to build the associated pharmacophore that should serve as a starting point for chemical modifications producing more active compounds. According to the obtained pharmacophore, it is not necessary to modify the indices of the atoms of the quinoxaline cycle. But the indices which would be modified to improve the anti-proliferative activity are those from the side chain.

References

[1] Skloot, R., The Immortal Life of Henrietta Lacks, Pan Macmillan, 2011.

[2] Scherer, W. F., Syverton, J. T., Gey, G. O., Studies on the propagation in vitro of poliomyelitis viruses. IV. Viral multiplication in a stable strain of human malignant epithelial cells (strain HeLa) derived from an epidermoid carcinoma of the cervix. *J. Exp. Med.* 1953, *97*, 695–710.

[3] Landry, J. J. M., Pyl, P. T., Rausch, T., Zichner, T., et al., The Genomic and Transcriptomic Landscape of a HeLa Cell Line. *G3 Genes Genomes Genet.* 2013, *3*, 1213–1224.

[4] Akhtar, J., Khan, A. A., Ali, Z., Haider, R., et al., Structure-activity relationship (SAR) study and design strategies of nitrogen-containing heterocyclic moieties for their anticancer activities. *Eur. J. Med. Chem.* 2017, *125*, 143–189.

[5] Akrami, H., Safavi, M., Mirjalili, B. F., Ashkezari, M. D., et al., Facile synthesis and antiproliferative activity of 7H-benzo[7,8]chromeno[2,3-d]pyrimidin-8-amines. *Eur. J. Med. Chem.* 2017, *127*, 128–136.

[6] An, W., Wang, W., Yu, T., Zhang, Y., et al., Discovery of novel 2-phenyl-imidazo[1,2-a]pyridine analogues targeting tubulin polymerization as antiproliferative agents. *Eur. J. Med. Chem.* 2016, *112*, 367–372.

[7] Hernández-Padilla, L., Vázquez-Rivera, D., Sánchez-Briones, L. A., Díaz-Pérez, A. L., et al., The Antiproliferative Effect of Cyclodipeptides from Pseudomonas aeruginosa PAO1 on HeLa Cells Involves Inhibition of Phosphorylation of Akt and S6k Kinases. *Molecules* 2017, *22*.

[8] Carta, D., Bortolozzi, R., Sturlese, M., Salmaso, V., et al., Synthesis, structure-activity relationships and biological evaluation of 7-phenyl-pyrroloquinolinone 3-amide derivatives as potent antimitotic agents. *Eur. J. Med. Chem.* 2017, *127*, 643–660.

[9] Cheng, W.-H., Shang, H., Niu, C., Zhang, Z.-H., et al., Synthesis and Evaluation of New Podophyllotoxin Derivatives with in Vitro Anticancer Activity. *Molecules* 2015, *20*, 12266–12279.

[10] Dandriyal, J., Singla, R., Kumar, M., Jaitak, V., Recent developments of C-4 substituted coumarin derivatives as anticancer agents. *Eur. J. Med. Chem.* 2016, *119*, 141–168.

[11] Diao, P.-C., Li, Q., Hu, M.-J., Ma, Y.-F., et al., Synthesis and biological evaluation of novel indole-pyrimidine hybrids bearing morpholine and thiomorpholine moieties. *Eur. J. Med. Chem.* 2017, *134*, 110–118.

[12] Li, F.-Y., Wang, X., Duan, W.-G., Lin, G.-S., Synthesis and In Vitro Anticancer Activity of Novel Dehydroabietic Acid-Based Acylhydrazones. *Molecules* 2017, *22*.

[13] Fytas, C., Zoidis, G., Tsotinis, A., Fytas, G., et al., Novel 1-(2-aryl-2-adamantyl)piperazine derivatives with antiproliferative activity. *Eur. J. Med. Chem.* 2015, *93*, 281–290.

[14] Gabr, M. T., El-Gohary, N. S., El-Bendary, E. R., El-Kerdawy, M. M., et al., Isatin-β-thiocarbohydrazones: Microwave-assisted synthesis, antitumor activity and structure-activity relationship. *Eur. J. Med. Chem.* 2017, *128*, 36–44.

[15] Gonçalves, B. M. F., Salvador, J. A. R., Marín, S., Cascante, M., Synthesis and anticancer activity of novel fluorinated asiatic acid derivatives. *Eur. J. Med. Chem.* 2016, *114*, 101–117.

[16] Li, W., Tan, G., Cheng, J., Zhao, L., et al., A Novel Photosensitizer 31,131-phenylhydrazine -Mppa (BPHM) and Its in Vitro Photodynamic Therapy against HeLa Cells. *Molecules* 2016, *21*.

[17] Żołnowska, B., Sławiński, J., Pogorzelska, A., Szafrański, K., et al., Novel 5-Substituted 2-(Aylmethylthio)-4-chloro-N-(5-aryl-1,2,4-triazin-3-yl)benzenesulfonamides: Synthesis, Molecular Structure, Anticancer Activity, Apoptosis-Inducing Activity and Metabolic Stability. *Molecules* 2016, *21*.

[18] Liu, Q., Li, W., Sheng, L., Zou, C., et al., Design, synthesis and biological evaluation of novel asperphenamate derivatives. *Eur. J. Med. Chem.* 2016, *110*, 76–86.

[19] Romagnoli, R., Baraldi, P. G., Prencipe, F., Oliva, P., et al., Design, synthesis and biological evaluation of 3-substituted-2-oxindole hybrid derivatives as novel anticancer agents. *Eur. J. Med. Chem.* 2017, *134*, 258–270.

[20] Levrier, C., Sadowski, M. C., Rockstroh, A., Gabrielli, B., et al., 6α-Acetoxyanopterine: A Novel Structure Class of Mitotic Inhibitor Disrupting Microtubule Dynamics in Prostate Cancer Cells. *Mol. Cancer Ther.* 2017, *16*, 3–15.

[21] Sun, B., Li, L., Hu, Q., Zheng, H., et al., Design, synthesis, biological evaluation and molecular modeling study of novel macrocyclic bisbibenzyl analogues as antitubulin agents. *Eur. J. Med. Chem.* 2017, *129*, 186–208.

[22] Xie, R., Yao, Y., Tang, P., Chen, G., et al., Design, synthesis and biological evaluation of novel hydroxamates and 2-aminobenzamides as potent histone deacetylase inhibitors and antitumor agents. *Eur. J. Med. Chem.* 2017, *134*, 1–12.

[23] Xia, Q.-H., Hu, W., Li, C., Wu, J.-F., et al., Design, synthesis, biological evaluation and molecular docking study on peptidomimetic analogues of XK469. *Eur. J. Med. Chem.* 2016, *124*, 311–325.

[24] Banu, S., Bollu, R., Bantu, R., Nagarapu, L., et al., Design, synthesis and docking studies of novel 1,2-dihydro-4-hydroxy-2-oxoquinoline-3-carboxamide derivatives as a potential anti-proliferative agents. *Eur. J. Med. Chem.* 2017, *125*, 400–410.

[25] Gregorić, T., Sedić, M., Grbčić, P., Paravić, A. T., et al., Novel pyrimidine-2,4-dione–1,2,3-triazole and furo[2,3-d]pyrimidine-2-one–1,2,3-triazole hybrids as potential anti-cancer agents: Synthesis, computational and X-ray analysis and biological evaluation. *Eur. J. Med. Chem.* 2017, *125*, 1247–1267.

[26] Karki, R., Jun, K.-Y., Kadayat, T. M., Shin, S., et al., A new series of 2-phenol-4-aryl-6-chlorophenyl pyridine derivatives as dual topoisomerase I/II inhibitors: Synthesis, biological evaluation and 3D-QSAR study. *Eur. J. Med. Chem.* 2016, *113*, 228–245.

[27] Pogorzelska, A., Sławiński, J., Żołnowska, B., Szafrański, K., et al., Novel 2-(2-alkylthiobenzenesulfonyl)-3-(phenylprop-2-ynylideneamino)guanidine derivatives as potent anticancer agents – Synthesis, molecular structure, QSAR studies and metabolic stability. *Eur. J. Med. Chem.* 2017, *138*, 357–370.

[28] Grozav, A., Porumb, I.-D., Găină, L. I., Filip, L., et al., Cytotoxicity and Antioxidant Potential of Novel 2-(2-((1H-indol-5yl)methylene)-hydrazinyl)-thiazole Derivatives. *Molecules* 2017, *22*.

[29] Gómez-Jeria, J. S., Abarca-Martínez, S., A theoretical approach to the cytotoxicity of a series of β-carbolinedithiocarbamate derivatives against prostatic cancer (DU-145), breast cancer (MCF-7), human lung adenocarcinoma (A549) and cervical cancer (HeLa) cell lines. *Pharma Chem.* 2016, *8*, 507–526.

[30] Gómez-Jeria, J. S., 45 Years of the KPG Method: A Tribute to Federico Peradejordi. *J. Comput. Methods Mol. Des.* 2017, *7*, 17–37.

[31] Hudson, R. F., Klopman, G., A general perturbation treatment of chemical reactivity. *Tetrahedron Lett.* 1967, *8*, 1103–1108.

[32] Klopman, G., Chemical reactivity and the concept of charge- and frontier-controlled reactions. *J. Am. Chem. Soc.* 1968, *90*, 223–234.

[33] Klopman, G., Hudson, R. F., Polyelectronic perturbation treatment of chemical reactivity. *Theor. Chim. Acta* 1967, *8*, 165–174.

[34] Peradejordi, F., Martin, A. N., Cammarata, A., Quantum chemical approach to structure-activity relationships of tetracycline antibiotics. *J. Pharm. Sci.* 1971, *60*, 576–582.

[35] Gómez Jeria, J. S., A new set of local reactivity indices within the Hartree-Fock-Roothaan and density functional theory frameworks. *Can. Chem. Trans.* 2013, *1*, 25–55.

[36] Gómez Jeria, J. S., Elements of Molecular Electronic Pharmacology, 1st ed., Ediciones Sokar, Santiago de Chile 2013.

[37] Gómez Jeria, J. S., Calculation of the Nucleophilic Superdelocalizability by the CNDO/2 Method. *J. Pharm. Sci.* 1982, *71*, 1423–1424.

[38] Gómez Jeria, J. S., La Pharmacologie Quantique. *Boll Chim Farm.* 1982, *121*, 619–625.

[39] Gomez-Jeria, J. S., On some problems in quantum pharmacology I. The partition functions. *Int. J. Quantum Chem.* 1983, *23*, 1969–1972.

[40] Gomez-Jeria, J. S., Cassels, B. K., Saavedra-Aguilar, J. C., A quantum-chemical and experimental study of the hallucinogen (±)-1-(2,5-dimethoxy-4-nitrophenyl)-2-aminopropane (DON). *Eur. J. Med. Chem.* 1987, *22*, 433–437.

[41] Gomez-Jeria, J. S., Morales-Lagos, D., Rodriguez-Gatica, J. I., Saavedra-Aguilar, J. C., Quantum-chemical study of the relation between electronic structure and pA2 in a series of 5-substituted tryptamines. *Int. J. Quantum Chem.* 1985, *28*, 421–428.

[42] Gómez-Jeria, J. S., Modeling the Drug-Receptor Interaction in Quantum Pharmacology, in: Maruani, J. (Ed.), *Molecules in Physics, Chemistry, and Biology*, Springer Netherlands, Dordrecht 1989, pp. 215–231.

[43] Gomez-Jeria, J. S., Sotomayor, P., Quantum chemical study of electronic structure and receptor binding in opiates. *J. Mol. Struct. THEOCHEM* 1988, *166*, 493–498.

[44] Gómez Jeria, J. S., Flores-Catalán, M., Quantum-chemical Modeling of the Relationships between Molecular Structure and In Vitro Multi-Step, Multimechanistic Drug Effects. HIV-1 Replication Inhibition and Inhibition of Cell Proliferation as Examples. *Can. Chem. Trans.* 2013, *1*, 215–237.

[45] Gómez Jeria, J. S., The use of competitive ligand binding results in QSAR studies. *Il Farm.* n. d., *40*, 299–302.

[46] Bruna-Larenas, T., Gómez-Jeria, J. S., A DFT and Semiempirical Model-Based Study of Opioid Receptor Affinity and Selectivity in a Group of Molecules with a Morphine Structural Core. *Int. J. Med. Chem.* 2012, 16.

[47] Gómez-Jeria, J. S., Castro-Latorre, P., A Density Functional Theory analysis of the relationships between the Badger index measuring carcinogenicity and the electronic structure of a series of substituted Benz[a]anthracene derivatives, with a suggestion for a modified carcinogenicity index. *Chem. Res. J.* 2017, *2*, 112–126.

[48] Gómez Jeria, J. S., Ovando-Guerrero, R., A DFT Study of the Relationships between Electronic Structure and Central Benzodiazepine Receptor Affinity in a group of Imidazo[1,5-a]quinoline derivatives and a group of 3-Substituted 6-Phenyl-4H-imidazo[1,5-a]-[1,4]benzodiazepines and related compounds. *Chem. Res. J.* 2017, *2*, 170–181.

[49] Kpotin, A. G., Atohoun, G. S., Kuevi, A. U., Houngue-Kpota, A., et al., A quantum-chemical study of the relationships between electronic structure and anti- HIV-1 activity of a series of HEPT derivatives. *J. Chem. Pharm. Res.* 2016, *8*, 1019–1026.

[50] Kpotin, G., Atohoun, S. Y. G., Kuevi, A. U., Kpota-Hounguè, A., et al., A Quantum-Chemical study of the Relationships between Electronic Structure and Trypanocidal Activity against Trypanosoma Brucei Brucei of a series of Thiosemicarbazone derivatives. *Pharm. Lett.* 2016, *8*, 215–222.

[51] Gómez-Jeria, J. S., Moreno-Rojas, C., Dissecting the drug-receptor interaction with the Klopman-Peradejordi-Gómez (KPG) method. I. The interaction of 2,5-dimethoxyphenethylamines and their N-2-methoxybenzyl-substituted analogs with 5-HT1A serotonin receptors. *Chem. Res. J.* 2017, *2*, 27–41.

[52] Kpotin, A. G., Kankinou, G., Kuevi, U., Gómez Jeria, J. S., et al., A Theoretical Study of the Relationships between Electronic Structure and Inhibitory Effects of Caffeine Derivatives on Neoplastic Transformation. *Int. Res. J. Pure Appl. Chem.* 2017, *14*, 1–10.

[53] Robles-Navarro, A., Gómez Jeria, J., A quantum-chemical analysis of the relationships between electronic structure and cytotoxicity, GyrB inhibition, DNA supercoiling inhibition and antitubercular activity of a series of quinoline–aminopiperidine hybrid analogues. *Pharma Chem.* 2016, *8*, 417–440.

[54] Frisch, M. J., Trucks, G. W., Schlegel, H. B., Scuseria, G. E., et al., G03 Rev. E. 01, Gaussian:, Pittsburgh, PA, USA 2007.

[55] Gómez Jeria, J. S., D-Cent-QSAR: A program to generate Local Atomic Reactivity Indices from Gaussian 03 log files. 1.0, Santiago de Chile 2014.

[56] Gómez-Jeria, J. S., An empirical way to correct some drawbacks of Mulliken Population Analysis (Erratum in: J. Chil. Chem. Soc., 55, 4, IX, 2010). *J. Chil. Chem. Soc.* 2009, *54*, 482–485.

[57] Gómez Jeria, J. S., Tables of proposed values for the Orientational Parameter of the Substituent. II. *Res. J. Pharm. Biol. Chem. Sci.* 2016, *7*, 2258–2260.

[58] Gómez Jeria, J. S., Tables of proposed values for the Orientational Parameter of the Substituent. I. Monoatomic, Diatomic, Triatomic, n-CnH2n+1, O-n-CnH2n+1, NRR', and Cycloalkanes (with a single ring) substituents. *Res. J. Pharm. Biol. Chem. Sci.* 2016, *7*, 288–294.

[59] Statsoft, Statistica 8.0, 2300 East 14 th St. Tulsa, OK 74104, USA 1984.